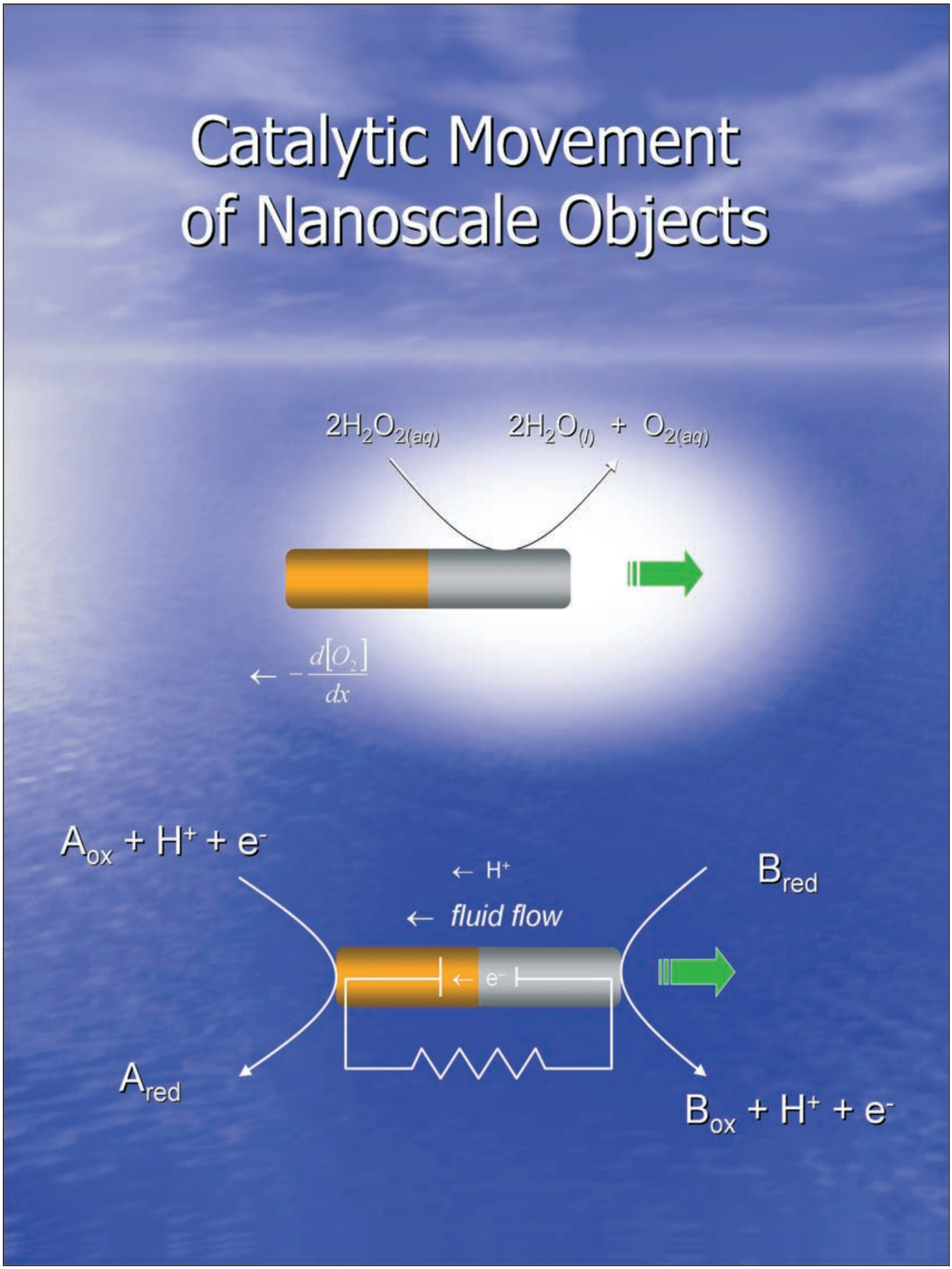

WILEY InterScience
© 2005 Wiley-VCH Verlag GmbH & Co. KGaA, Weinheim

DOI: 10.1002/chem.200500167

Motility of Catalytic Nanoparticles through Self-Generated Forces

Walter F. Paxton, Ayusman Sen,* and Thomas E. Mallouk*[a]

Abstract: Small-scale synthetic motors capable of generating their own motive forces by exploiting the chemical free energy of their environment represent an important step in developing practical nanomachines. Catalytic particles are capable of generating concentration and other gradients that can be used to self-propel small objects. However, the autonomous movement of catalytic nanoparticles by self-generated forces is a relatively unexplored area in colloid and interfacial chemistry. This paper explores the potential of catalytically self-generated forces for propulsion of small objects through fluids.

Keywords: colloids · heterogeneous catalysis · motion · nanotechnology · self-electrophoresis

Introduction

Control over the movement of matter on the micron, submicron, and nanometer length scales is an important objective in science and engineering. There is a practical motivation for studying this problem, because it would be desirable for many applications to be able to make tiny machines of different kinds. However, scaling of conventional machine designs to micron and submicron dimensions, and providing these machines with power are both daunting tasks. There is also a fundamental reason for attaining a better understanding of the principles that govern motion on the micron and nanometer regimes in fluids. Although many of these principles are fairly well understood in general, some specific questions about the mechanisms of cell motility, biologically derived molecular motors, and interfacial phenomena remain unanswered. While there have been several important advances and discoveries in each of these areas, the ability to artificially stimulate and control the movement of individual small objects dispersed in fluids remains a relatively unexplored problem at the interface of many disciplines. Solutions to this problem would accelerate scientific achievement in a variety of fields including biology, medicine, and emerging nanotechnology.

Biological systems produce the smallest and some of the most complex motors known. These protein nanomotors provide the forces that perform many important biological functions that include ATP synthesis, bacterial motility, cell replication, intracellular transport, and skeletal muscle contraction.[1] Some of these biologically derived motors have been studied extensively as researchers develop useful applications and seek to understand the mechanisms by which they operate. While the mechanisms vary, a common principle is the use of catalysis to convert the chemical free energy of the environment into useful work. Although the work of these motors is coordinated through complicated mechanistic pathways, individual protein motors are able to harvest local chemical energy independent of one another and operate autonomously.

In contrast, most nonbiological approaches to moving small objects through fluids involve externally applied fields generated from macroscale sources. Several types of fields have been used in this manner including magnetic,[2,3] electric,[4] thermal,[5–7] and concentration fields.[8–10] While magnetic field gradients act on the body of a magnetic particle, electric, thermal, and concentration fields act on the interfacial region between a particle and the fluid to induce translational movement relative to the surrounding fluid. Anderson's review of these interfacial forces includes relationships for the observed velocity of a particle moving in response to linear external fields.[11] These types of field-induced movement require either macroscale power supplies or external chemical reservoirs in order to maintain fields sufficient to move small objects. In addition, field-induced effects act on all objects within the field, resulting in an ensemble behavior of similar suspended particles, rather than particles moving independent of one another. These two characteris-

[a] W. F. Paxton, Prof. Dr. A. Sen, Prof. Dr. T. E. Mallouk
Department of Chemistry
The Pennsylvania State University
104 Chemistry Research Building
University Park, PA 16802(USA)
Fax: (+1) 814-863-9637
E-mail: asen@chem.psu.edu
tom@chem.psu.edu

 © 2005 Wiley-VCH Verlag GmbH & Co. KGaA, Weinheim

tics make field-induced movement of particles an efficient strategy for sorting of particles based on their behavior in an applied field, but unattractive for synthetic autonomous motors.

An interesting question arises when we consider a particle that creates its *own* gradient by using the chemical free energy of its environment. Macroscale examples of this type of phenomenon are well known, for example, the spontaneous movement of a camphor scraping on water.[12,13] Motion in this case is attributed to the asymmetric dissolution of camphor in water resulting in a concentration-gradient-induced surface stress. Sano et al. studied the behavior of mercury drops in acidic potassium dichromate solutions,[14] attributing the observed motion to an asymmetric interfacial tension gradient caused by the reaction of a mercury drop with the oxidizing solution. More recently, Whitesides et al. have used a platinum catalyst to drive millimeter-scale plastic disks across a hydrogen peroxide containing water surface,[15] and Mitsumata et al. demonstrated the use of chemical-gradient-based motion to fabricate a motor powered by the dissolution of a solvent in an aqueous solution.[16] In each case, spontaneous motion was induced by gradients, which were generated by an interaction of the object with its surroundings.

Each of the above examples are the result of chemical or physical reactions in which the moving object supplies the necessary "fuel" required to induce movement, the exception being the Whitesides experiment for which a catalyst was used as the "engine". Catalytic engines are attractive for nanoscale devices, because they circumvent the need for the moving object to store required fuel "on board", instead allowing the chemical free energy of the system to be released at spatially-defined catalytic sites. As a result of these localized areas of activity, catalyst particles naturally create chemical gradients due to the consumption of reactants and appearance of the products at the particle/fluid interface. In the case of a symmetrical particle, the net force due to gradients generated by the particle essentially cancels out by symmetry. On the other hand, the active site of an asymmetric catalytic particle (e.g., one that is catalytic on only one side) creates a gradient by reacting with a substrate "fuel" that is supplied locally. The resulting gradient can then act on the noncatalytic surface of the particle to produce motion.

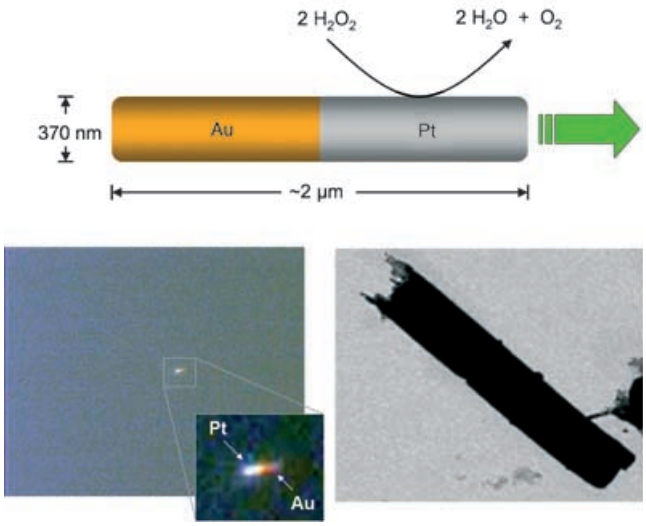

Figure 1. Platinum/gold nanorods composite: Top: Schematic of a platinum/gold nanorod (from reference [17], Copyright 2004 American Chemical Society). Bottom left: An optical micrograph (500×) of a platinum/gold rod. Bottom right: Transmission electron micrograph of a platinum/gold rod.

Proof of Concept

We have demonstrated this concept by using asymmetric catalytic particles to self-generate gradients capable of inducing movement, using the platinum-catalyzed decomposition of hydrogen peroxide as the principal reaction.[17] We electrochemically fabricated metal nanorods consisting of a platinum and a gold segment (Figure 1) that move in their axial direction at speeds up to 30+ microns per second when placed in hydrogen peroxide solutions. Interestingly, these nanorods move with the platinum end forward, which is in contrast to the direction of motion in the macroscale experiment of Whitesides et al, in which the platinum catalyst providing the propulsive force was at the trailing end of the moving object.[15] Movement along the long axis of the rods is expected because the catalytic reaction results in an asymmetric concentration gradient along the noncatalytic end of the rod. In addition to the observed linear motion of individual rods, aggregates of two or more rods typically exhibit rotational motion. This rotational behavior was observed for platinum–gold rods (Figure 2; see also Supporting Information from reference [17]), and subsequently for nickel nanorods by Ozin et al.[18] Although the decomposition of hydrogen peroxide results in the formation of oxygen gas, bubbles typically do not nucleate on the smooth metal surfaces of the rods, allowing us to observe their movement directly by optical microscopy.

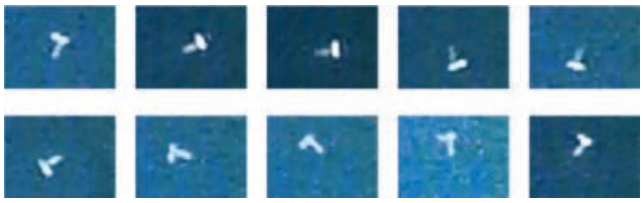

Figure 2. Cooperative rotational motion of T-shaped assemblies of platinum/gold rods in 2.5% aqueous hydrogen peroxide.[17] Each frame represents 0.1 s, and the assembly rotates approximately once per second. Similar rod rotors have recently been reported by Ozin et al.[18]

By comparing the hydrogen peroxide concentration to the average observed rod velocity, we confirmed the relationship between the two (Table 1). Furthermore, we found that

 © 2005 Wiley-VCH Verlag GmbH & Co. KGaA, Weinheim

Table 1. Effect of aqueous H_2O_2 concentration on the movement of 2 μm long Pt/Au rods. Concentration of rods: 3.3×10^7 rods mL^{-1}. Error limits represent 90% confidence interval.

H_2O_2 [wt%]	Speed [μm s^{-1}]	Directionality ($\tau=0.1$ s)	Axial velocity [μm s^{-1}]
4.9	7.7 ± 0.9	0.78	6.6 ± 1.0
3.3	7.9 ± 0.7	0.75	6.6 ± 0.7
1.6	5.6 ± 0.6	0.65	4.0 ± 0.8
0.33	4.9 ± 0.3	0.60	3.4 ± 0.4
0.031	3.9 ± 0.5	0.19	0.9 ± 0.4
pure water	3.7 ± 0.3	0.07	0.4 ± 0.1

the experimental rate of oxygen formation from 3.7% hydrogen peroxide was approximately 1/2000 of the limit imposed by the hydrogen peroxide diffusion rate, implying that the rate of oxygen production is limited by the surface area of the catalytic platinum segment.

Mechanism

While it may make intuitive sense that a particle with chemical reactions taking place asymmetrically on its surface would exhibit self-propulsion, the mechanism by which chemical energy is converted to mechanical energy is less obvious. Although it is tempting to attribute the movement to a single source, it is possible that there may be several cooperating and even opposing effects that result in the observed movement. An examination (and estimation, where possible) of these effects should allow us to determine the primary factor(s) responsible for the observed self-propulsion of bimetallic rods in hydrogen peroxide solutions. It could also in principle allow one to design catalytic nanomotors that are propelled by different mechanisms. We have explored a number of possibilities, including: differential pressure, diffusiophoresis, interfacial tension, and self-electrophoresis.

From the balanced equation for the decomposition of hydrogen peroxide, $2H_2O_2\rightarrow2H_2O+O_2$, the stoichiometric ratio of products to reactants is 3:2. Because this reaction is fast and takes place only on one end of the rod, it is conceivable that the increase in number of molecules on the catalytic end of the rod could lead to pressure-driven flows, pushing the particle from the region of high pressure (catalyst end) to low pressure. However, this pressure-driven or "thrust" mechanism cannot be the dominant propulsive force, because the pressure gradient described would push the rod towards the gold segment, which is opposite to the movement observed.

Although a pressure gradient is unlikely to be the primary effect, a concentration gradient would certainly be established. It is well known that chemical, temperature, or other gradients can induce phoretic movement of a colloidal particle, and the resulting slip velocity exhibited in these systems can be described as a product of some constant (b) and the undisturbed gradient ($\bigtriangledown Y_\infty$). Our experiment most simply and closely resembles a diffusiophoretic system,[11] and we considered the effects of a gradient of neutral solute molecules (O_2) in generating forces along the axis of the rods. For diffusiophoretic systems we can write Equation (1) in which KL^* is a parameter describing the characteristics of the solute.

$$b=\frac{kT}{\eta}KL^* \tag{1}$$

By modeling the dioxygen molecules as hard spheres, this product can be estimated by Equation (2) in which a is the radius of the dioxygen molecule ($\sim1\times10^{-10}$ m).

$$KL^*=-\frac{a^2}{2} \tag{2}$$

The oxygen concentration gradient, dc/dx, was estimated from Fick's law for mass flux [Eq. (3)] in which J is the surface-normalized oxygen evolution rate ($\sim7.7\times10^{-4}$ mol O_2 m^{-2}, based on measured $9.7(4)\times10^{-16}$ mol O_2 s^{-1} per rod and a platinum segment surface area of 1.3×10^{-12} m^2) and D is the dioxygen diffusion coefficient (2.42×10^{-5} cm^2 s^{-1}) to give a concentration gradient at the surface of the rod of -3.2×10^5 mol O_2 m^{-4} (-3.2×10^{-3} mol O_2 cm^{-4}).

$$\frac{dc}{dx}=-\frac{J}{D} \tag{3}$$

Using the expression for slip velocity due to diffusiophoresis, the predicted velocity is 4 nm s^{-1} along the O_2 gradient. Thus, the diffusiophoretic model predicts a velocity much smaller than that observed and in the wrong direction.

Interfacial tension gradients that arise in response to temperature or chemical gradients offer another interesting possibility. The decomposition of hydrogen peroxide is exothermic (ΔH^o on the order of -200 kJ mol^{-1}), creating both oxygen concentration and thermal gradients. Because the source of the gradients is the rod itself (i.e., the platinum end of the rod), the gradients that act on the length of the gold end are continually re-established as it moves through solution as long as hydrogen peroxide is present. An important question is whether or not the minute changes in temperature and chemical composition are sufficient to generate the forces necessary to move micro- and nanoscale objects. The force impelling the rods is balanced by the drag due to movement through a viscous fluid and may be estimated using Stokes drag law for a cylinder[19] [Eq. (4)], which predicts an opposing propulsive force of ~0.048 pN for a 2 μm long rod moving 10 μm s^{-1}.

$$F_{drag}=\frac{2\pi\mu L}{\ln\left(\frac{2L}{R}\right)-0.72}v \tag{4}$$

The work due to changes in interfacial tension or surface expansion can be expressed in terms of surface area (σ) and interfacial tension (γ) [Eq. (5)].

 © 2005 Wiley-VCH Verlag GmbH & Co. KGaA, Weinheim

$$dW = \gamma\, d\sigma + d\gamma\, \sigma \tag{5}$$

Because the surface area of the particle is constant, we can neglect the first term. By symmetry, γ only changes in the x direction (along the length of the rod) and the force on a thin slice of the cylinder with circumference $2\pi R$ and thickness dx is given by Equation (6), which can be integrated to give Equation (7).

$$dF = \frac{d\gamma}{dx} 2\pi R\, dx \tag{6}$$

$$F = \int \frac{d\gamma}{dx} 2\pi R\, dx = \Delta\gamma\, 2\pi R \tag{7}$$

(Note that this neglects the surface area of the rod ends which accounts for $<10\,\%$ of rod surface area.) Using this expression, the interfacial tension difference required to balance the drag force based on experimental data ($R=185$ nm; $F=0.048$ pN) is 4.1×10^{-5} mN m^{-1}. Thus an interfacial tension difference of only 4.1×10^{-5} mN m^{-1} (0.041 pN μm^{-1}) is sufficient to move a rod through solution.

While it is experimentally very difficult to measure the relevant solid–liquid interfacial tensions present in our system, an order of magnitude approximation can be made by what we do know about temperature and chemical composition effects on the interfacial tension at the liquid–vapor interface. The chemical gradient present arises from the balance of oxygen production and diffusion, and may be estimated by solving the convection–diffusion equation for our system.[17] The resulting concentration difference from one end of the rod to another may be written as Equation (8) in which S is the surface normalized oxygen evolution rate, R and L the rod radius and length, and D the diffusion coefficient of oxygen.

$$\Delta C \approx \frac{SR}{2D} \ln\left(\frac{L}{2R}\right) \tag{8}$$

This concentration difference can be related to interfacial tension as the mole-fraction-weighted average of the component interfacial tensions[20] [Eq. (9)].

$$\gamma_{AB} = \gamma_A \chi_A + \gamma_B \chi_B \tag{9}$$

As noted above, the interfacial tension difference need only be 4.1×10^{-5} mN m^{-1} (0.041 pN μm^{-1}) to provide the necessary force. Using the linear approximation for interfacial tension, and taking the interfacial tension of oxygen gas to be ~0, this corresponds to a concentration difference of 3.1×10^{-5} M. Based on our observed oxygen evolution rate and the dimensions of our rods, the molar concentration difference is 6.6×10^{-5} M over 1 μm for rods in 3.7 % hydrogen peroxide, which is sufficient to produce force of the appropriate magnitude. By contrast, modeling the temperature flux from the platinum surface with the convection–diffusion equation, the thermally induced change in interfacial tension generates a net forward force on the order of 10^{-4} pN; that is, two orders of magnitude smaller than that required to balance the drag force.[17]

According to the chemical (O_2) gradient-induced interfacial tension effect, the steady-state velocity for bimetallic rods with large aspect ratios $L/2R>5$ should scale approximately as Equation (10) in which S is the surface area normalized oxygen generation rate, γ is the solution-solid interfacial tension, μ is the viscosity, D is the diffusion coefficient of oxygen in water, R is the radius, and L is the length of the rod.

$$v_z \propto \frac{S\gamma R^2}{\mu D L} \tag{10}$$

The interfacial tension may be modified by adding another miscible component, such as ethanol, to the system. In addition to changing the tension of the fluid at the liquid–vapor (and presumably the liquid–solid) interface, ethanol also affects the oxygen evolution rate, but the rod velocity should scale as the product of these two parameters. Figure 3 shows a plot of average velocity versus the product

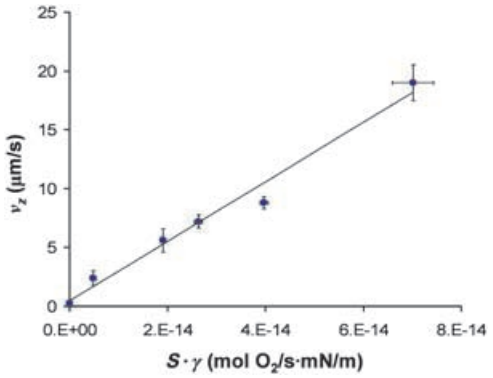

Figure 3. Plot of speed versus $S\gamma$. The effect of ethanol on axial velocity (v_z), whereby v_z is plotted versus the product of oxygen evolution rate per rod (S) and solution surface tension γ (from reference [17], copyright 2004 American Chemical Society).

$S\gamma$ for a sample of rods solutions of hydrogen peroxide in ethanol–water mixtures. The plot is linear, as expected from Equation (10). The addition of ethanol also affects μ and D, but according to the Stokes–Einstein equation the product of these two parameters is approximately constant, and thus these two effects balance each other.

While the interfacial tension effect described above predicts force of the appropriate magnitude, it does not address the direction of rod movement. If this effect is responsible for the observed movement, a hydrophilic rod should move down the interfacial tension gradient in order to minimize the surface free energy of the system. The fact that the rods move with their platinum ends forward suggests that the surface free energy is minimized as the gold end "swims" up the oxygen concentration gradient, which in turn suggests

 © 2005 Wiley-VCH Verlag GmbH & Co. KGaA, Weinheim

that the gold is hydrophobic. The hydrophobicity of the gold may arise from surface impurities[21] or nanoscopic air cavities pinned to the surface of the gold, as reported in the literature.[22,23] Atomic force microscopy images of platinum/gold particles in pure water confirm the presence of nanobubbles and explain the direction of movement.[17]

Self-Electrophoresis

One final possibility currently under investigation is that of self-electrophoresis, which could result from electrochemical hydrogen peroxide decomposition at both the platinum *and* gold ends of a moving rod. This problem is similar to that of a hypothetical biological cell that uses active transport to pump ions (or neutral solute) into the cell on one end and out at the other, an idea considered theoretically by Anderson[11] and by Lammert et al.[24] Such a cell would be capable of maintaining a dynamic electric field (and/or concentration gradient) tangential to the cell surface. This gradient would be superimposed over the cell's equilibrium double layer by the continuous pumping of ions. Ions (or solute) in the double layer would migrate in response to this dynamic electric field, resulting in fluid flow in the interfacial region between the cell membrane and the surrounding fluid and a corresponding slip velocity.

Similarly, a conducting colloidal particle that catalyzes an oxidation reaction on one end and a reduction reaction on the other would generate its own ion gradient. Consider an asymmetric conducting particle with two ends that catalyze two different electrochemical half reactions under acidic conditions[25] [Eqs. (11) and (12)], such that both oxidized and reduced species are neutral, $E_1 + E_2$ is positive (i.e., the reaction is spontaneous), and the overall reaction on the particle surface is fast (Figure 4).

$$A_{red} \rightarrow H^+ + e^- + A_{ox} \qquad E_1 \tag{11}$$

$$B_{ox} + H^+ + e^- \rightarrow B_{red} \qquad E_2 \tag{12}$$

Note that the reaction would proceed with a flux of electrons *inside* the particle, as well as the migration of protons

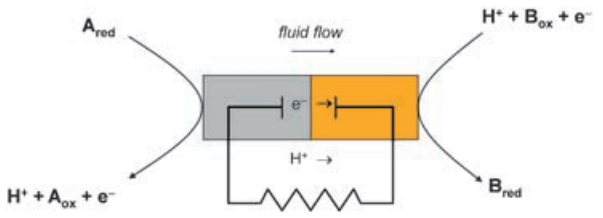

Figure 4. Redox active particle capable of generating its own electric field. Species A is catalytically oxidized on one side, generating a proton and an electron that are consumed when B is catalytically reduced on the opposite side. The asymmetric production and consumption of ions results in a concentration polarization induced electric field driven by the net reduction of free energy. Ions adjacent to the surface migrate in response to the electric field.

outside the particle from one end to the other. In this way, the particle effectively acts as a short-circuited galvanic cell with the electron current (and corresponding ion current) being driven thermodynamically by the net reduction of chemical free energy.

From the balanced half-reactions, the electron current through the particle is equal to the ion current in the fluid surrounding the particle, $i_{e^-} = i_{M^+} - i_{X^-}$, and the related current densities are then given by $J = i_{e^-}/A_{flux}$, in which A_{flux} is the cross-sectional area through which the electrons or ions flow. This area for the electron flux is the cross-sectional area of the particle, and the ion flux primarily occurs in the electrical double layer surrounding the particle in water (Figure 5), the thickness of which is given by the Debye length [Eq. (13)].

$$\lambda_D = \frac{9.61 \times 10^{-9}}{(Ic)^{1/2}} \tag{13}$$

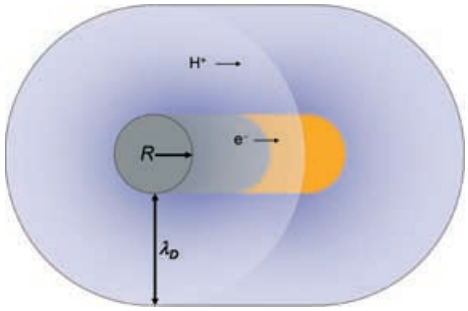

Figure 5. The flux of electrons (e^-) through the particle with cross sectional area with radius (R) is balanced by the flux of ions (H^+) through the double layer with thickness λ_D on the outside of the particle.

Here I is the ionic strength of the solution and c is the molarity of the dilute electrolyte solution in $mol\,m^{-3}$. The electric field (E) generated by the flux of electrons or ions (J) can then be estimated from Ohm's Law, $E = J/\sigma$, in which σ is the conductivity of the charge transport medium. The conductivity of the particle itself is very high ($> 10^5\,S\,m^{-1}$ for a metal particle), but the double-layer conductivity is much smaller ($< 10^{-5}\,S\,m^{-1}$),[26] meaning that the electric field established in the particle double layer can be up to 10^{10} times greater than that in the particle itself.

Because the ions in the double layer migrate with respect to the particle surface in response to this self-generated electric field, by Galilean invariance the particle moves with respect to the fluid. As in the case of external electrophoresis, the observed slip velocity would be a linear function of the electric field, which is a function of the current in, and conductivity of, the interfacial double-layer region. Assuming classical behavior, the particle should migrate in its self-generated electric field according to the Hückel equation for electrophoretic slip velocity in the limit of large Debye length [Eq. (14)].

 © 2005 Wiley-VCH Verlag GmbH & Co. KGaA, Weinheim

$$v = \frac{2}{3}\frac{\varepsilon_0 \varepsilon \zeta E_x}{\mu} \quad (14)$$

Furthermore, the electric field parallel to the particle surface (E_x) can be written in terms of the ion current density and the two-dimensional double-layer conductivity. Assuming that the dominant charge carriers are cations in the double layer adjacent to the negatively charged metal surface, we obtain Equation (15).

$$v = \frac{2}{3}\frac{\varepsilon_0 \varepsilon \zeta}{\mu}\frac{J_{M^+}}{K_\lambda^{od}} \quad (15)$$

Using this relation, a particle with a zeta potential of -40 mV requires an ion current density of only 5×10^{-4} mA cm^{-2} to move 10 μm s^{-1}. Thus, electrohydrodynamic fluid pumping due to a catalytic redox couple can in principle propel a rod through solution.

Designing particles with orthogonal but complementary redox properties presents an interesting challenge. One end of the particle would have to be an efficient oxidation catalyst, but an inefficient reduction catalyst. The reverse would be true for the other end (i.e., a good reduction and a poor oxidation catalyst), and the two catalytic ends would need to be in electrical contact with one another through the particle to allow current to flow. Finally, the reaction would need to be fast enough to generate field strengths necessary for particle movement. By the Hückel approximation, the electric field required to move a micron-sized colloidal particle with an electrokinetic zeta potential of -40 mV in pure water at a speed of 10 μm s^{-1} is on the order of 500 V m^{-1}. However, electric fields scale with length, and a 500 V m^{-1} field corresponds to a potential difference of only 0.5 mV over a 1 μm long particle.

Reactions that meet the above criteria may be found in the fuel cell literature, such as the electrochemical oxidation of hydrogen or methanol coupled with the reduction of oxygen; this reaction proceeds at relatively moderate temperatures and pressures.[27] Although a platinum catalyst can be used as both the anode and the cathode, recent advances have used Pt alloys to optimize either the anode or cathode efficiency. For example, Pt/Co and Pt/Pd alloys are more active for the reduction of oxygen than platinum alone.[28,29] Conversely, Pt/Ru catalysts exhibit higher activity and longer lifetimes than platinum alone when used as a hydrogen- or methanol-reducing catalyst,[30] and electrodeposition of these platinum containing alloys has been demonstrated.[31,32] Approaches to alloy formation may then be applied to template-based methods to fabricate metallic nanorods with alloy segments and tested for motility in fuel solutions by means of optical microscopy. Work is currently underway to explore these and other possibilities.

While the speed of Au/Pt nanorods propelled in this manner is comparable to that of flagellar bacteria, the energy conversion efficiency of the former is very small (on the order of 10^{-9}).[33] In contrast, biological energy transduction is quite efficient, often greater than 50%. While biological motors use less exoergic reactions, such as ATP hydrolysis, the main reason for their efficiency is the intimate, atomic-level mechanical coupling of the catalyst with the reactants/products. We believe that energy conversion efficiencies orders of magnitude higher than that of the Au/Pt nanorod–H_2O_2 system could be achieved by bearing this principle in mind. This is an exciting prospect because even the very inefficient energy conversion we have so far achieved is capable of generating forces that can turn gears and outrun certain unicellular organisms. Increasing the efficiency by even two orders of magnitude (to 10^{-7}) would give us much faster motion on the bacterial-length scale, and would allow us to make much smaller nanomotors according to the scaling law in Equation (10).

Current and Future Work

Because small, moving particles are subject to rotational Brownian motion, the movement of catalytic particles due to self-generated gradients is unidirectional, but still somewhat random. In addition to inducing movement, control over the direction this motion is important for developing functional devices. One approach to harnessing the catalytically induced movement of nanorods is to use externally applied magnetic fields. Segments of magnetic metals are easily incorporated into electrochemically grown nanorods, allowing one to fabricate particles that are both catalytically and magnetically active. Kline et al. demonstrated this by making platinum/gold rods that included nickel segments, which were subsequently magnetized (Figure 6).[34] These particles exhibited normal autonomous movement in hydrogen peroxide solutions, but they also oriented in, and moved perpendicular to, an applied magnetic field. Manipulation of the applied field allowed the nickel-containing rods to be remotely steered through the solution with micron-scale precision. Because the rods oriented and moved perpendicular to the magnetic field, this field served only to align the rods and not to provide an additional propulsive force. Thus the rods were driven by the catalytic decomposition of hydrogen

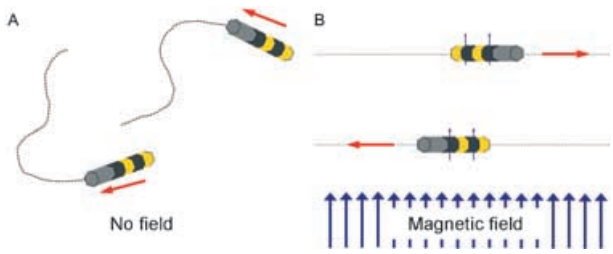

Figure 6. Platinum/gold rods with short, magnetized nickel segments (length < diameter). A) These rods move autonomously in hydrogen peroxide solution, but are still subject to rotational thermal energy resulting in autonomous but undirected motion. B) When an external magnetic field is applied, particles align and move perpendicular to the applied field. The particles are driven by the catalytic decomposition of hydrogen peroxide and directed by the application of an external field (from reference [35]).

 © 2005 Wiley-VCH Verlag GmbH & Co. KGaA, Weinheim

peroxide and were remotely steered by the externally applied magnetic field.

Another approach to controlling the movement of catalytic objects is to design rotary motors that could be harnessed to drive an array of gear assemblies. Catchmark et al. have fabricated 150 μm diameter gold "gears" with platinum deposited on one side of each tooth (Figure 7).[35] These gears rotate once per second when placed in dilute hydrogen peroxide solutions, which corresponds to a linear speed of ~390 $\mu m\,s^{-1}$. These gears may ultimately be attached to a surface-bound shaft adjacent to other structures to provide useful work.

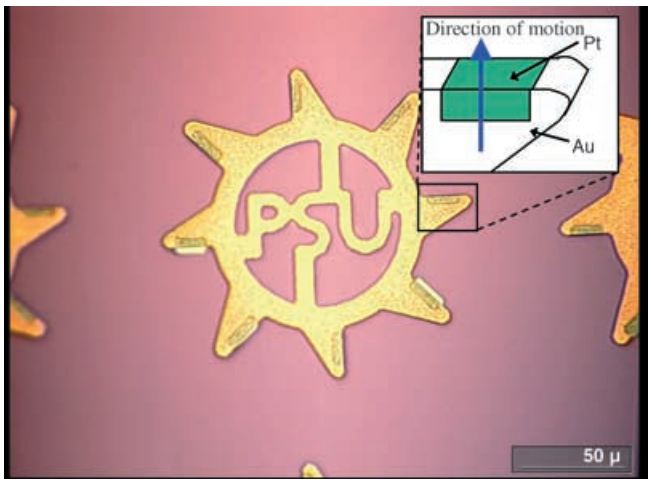

Figure 7. Microfabricated gold "gears" with platinum on one side of each of the teeth. The result is the counterclockwise rotation of the structure when placed in hydrogen peroxide solution (from reference [35]).

These demonstrations of autonomous motion of catalytically asymmetric objects represent an effort to understand and induce movement on the microscale. Although the examples above use platinum as the catalyst, other hydrogen peroxide decomposition catalysts, such as nickel,[18] exhibit the same effect. In principle, any reaction that occurs on asymmetric catalytic particles will also result in gradients capable of inducing particle movement. This has some interesting implications for bionanotechnology, because enzymes asymmetrically bound to small particles (or expressed asymmetrically on cell surfaces) could induce gradient-based motility. Photocatalytic reactions could also be incorporated into these systems to allow the motility of particles to be turned on and off with an external light source. Finally, polymerization catalysts immobilized asymmetrically on a micro/nanoparticle surface could impel the particle through solution, mimicking the actin polymerization-based motility of lysteria[36] and other nonflagellar motile bacteria.

One fascinating aspect of independently moving small objects is that they provide the first synthetic analogues of motile bacteria. The movement of platinum/gold rods in hydrogen peroxide bears a striking resemblance to nonflagellar swimming synechococcus cyanobacteria,[37] and the magnetic moment of nickel-containing motile nanorods are on the same order as that of magnetotactic bacteria ($\sim 1\times 10^{-15}\,A\,m^2$).[34,38] These synthetic analogues may allow researchers to explore aspects of cell motility and chemotaxis by subjecting the more robust inorganic moving particles to a wider range of experimental conditions than are possible with living cells. For example, the chemotactic responses of *E. coli* and related multiflagellar bacteria involve a "memory" effect of a few seconds that increases the time between directional changes as the bacteria swim into a chemoreceptor concentration gradient.[39] In the inorganic system, this memory effect might be mimicked by the slow adsorption/desorption of a catalyst inhibitor, and parameters such as temperature could be changed to study the kinetics and thermodynamics of the process. It is interesting to note that it is possible to make controlled aggregates or "rafts" of metallic nanorods through different techniques such as magnetic aggregation,[40] linking with DNA,[41] or noncovalent assembly.[42] With these rafts, chemotactic "steering" might be possible, as illustrated in Figure 8.

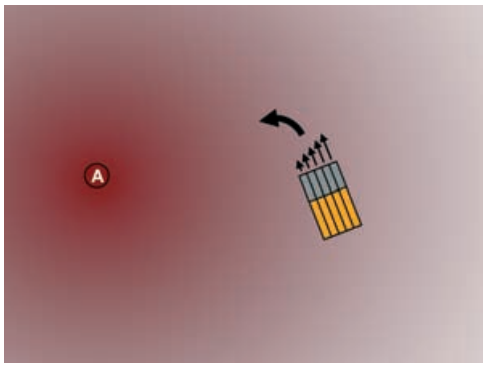

Figure 8. Schematic drawing of a raft of catalytic nanomotors illustrating a possible chemotactic response. The raft is immersed in a fuel solution that contains a source (A) of inhibitor molecules, which bind reversibly the surface of the catalyst stripes. The corner of the raft closest to the inhibitor source moves slower than the far corner, causing the raft to turn towards the source. The velocity of raft motion should decrease as it approaches the source.

In addition to providing a robust synthetic analogue of motile bacteria, nano/micro objects designed with gradient-generating catalysts as the motors could perform a variety of useful functions. At this point it is quite possible to drive a micron-sized motor to a microscopically specific location, the propulsion arising from the catalytic motor and the direction being controlled by magnetism.[34] These motors could be designed with functional regions to analyze their environment, shuttle cargo to and from specific areas, or assemble and disassemble nanostructures. One could envision a biologically compatible motor equipped with a sensor to determine information about its immediate environment, or one that could perform microsurgical operations such as removing cancerous cells at or delivering medicine to precise areas of a living organism.

 © 2005 Wiley-VCH Verlag GmbH & Co. KGaA, Weinheim

While in principle the autonomous movement of catalytically asymmetric particles has great potential, their utility and practicality remains to be seen. At the very least, these first-generation structures demonstrate the fulfillment of the most fundamental requirements of nanomachinery: initiation of and control over motion. The attainment of the functional objectives (sensing, shuttling, and nanoconstructing) will require a great deal of rational or fortuitous progress. Several priorities will be the likely focus of work in our laboratory and others in the near term. These include exploring in more detail the mechanism of catalyzed motion by using different reactions and broadening the class of catalytic reactions that can induce motion, in particular to biocompatible fuels such as glucose. This increased understanding will enable the design of more energy efficient nanomotors with a broader range of possible applications.

Acknowledgements

We gratefully acknowledge the intellectual contributions of our collaborators on this project, in particular Timothy Kline, Jeffrey Catchmark, Paul Lammert, Vincent Crespi, Shyamala Subramanian, Shakuntala Sundararajan, Yanyan Cao, and Yang Wang. We also thank Blake Peterson, Darrell Velegol, Jason Gestwicki, and David Vanderbilt for very helpful discussions on the mechanisms and applications of catalyzed motion on the nanoscale. This work is supported by the Penn State Center for Nanoscale Science, which is funded by NSF grant DMR-0213623.

[1] M. Schliwa, G. Woehlke, *Nature* **2003**, *422*, 759–765.
[2] T. M Vickrey, J. A. Garcia-Ramirez, *Sep. Sci. Technol.* **1980**, *15*, 1297–1304.
[3] H. Watarai, M. Suwa, Y. Iiguni, *Anal. Bioanal. Chem.* **2004**, *378*, 1693–1699.
[4] *Interfacial Electrokinetics and Electrophoresis* (Ed.: Á. V. Delgado), Dekker, New York, **2002**.
[5] B. V. Derjaguin, N. V. Churev, V. M. Muller, *Surface Forces* (Engl. transl.), Consultants Bureau, New York, **1987**.
[6] K. J. Zhang, M. E. Briggs, *J. Chem. Phys.* **1999**, *111*, 2270–2282.
[7] R. Piazza, *J. Phys. Condens. Matter* **2004**, *16*, S4195–S4211.
[8] M. M. Lin, D. C. Prieve, *J. Colloid Interface Sci.* **1983**, *95*, 327–339.
[9] J. P. Ebel, J. L. Anderson, D. C. Prieve, *Langmuir*, **1988**, *4*, 396–406.
[10] H. J. Keh, Y. K. Wei, *Colloid Polym. Sci.* **2000**, *270*, 539–546.
[11] J. L. Anderson, *Annu. Rev. Fluid Mech.* **1989**, *21*, 61–99.
[12] L. Raleigh, *Proc. R. Soc. London* **1890**, *47*, 364.
[13] S. Nakata, S. Hiromatsu, H. Kitahata, *J. Phys. Chem. B* **2003**, *107*, 10557–10559.
[14] O. Sano, K. Kutsumi, N. Watanabe, *J. Phys. Soc. Jpn.* **1995**, *64*, 1993–1999.
[15] R. F. Ismagilov, A. Schwartz, N. Bowden, G. M. Whitesides, *Angew. Chem.* **2002**, *114*, 674–676; *Angew. Chem. Int. Ed.* **2002**, *41*, 652–654.
[16] T. Mitsumata, J. P. Gong, Y. Osada, *Polym. Adv. Technol.* **2001**, *12*, 136–150.
[17] W. F. Paxton, K. C. Kistler, C. C. Olmeda, A. Sen, S. K. St. Angelo, Y. Cao, T. E. Mallouk, P. E. Lammert, V. H. Crespi, *J. Am. Chem. Soc.* **2004**, *126*, 13424–13431.
[18] S. Fournier-Bidoz, A. C. Arsenault, I. Manners, G. A. Ozin, *Chem. Commun.* **2005**, 441–443.
[19] J. Happel, H. Brenner, *Low Reynolds Number Hydrodynamics*, Prentice Hall, Englewood Cliffs, NJ, **1965**, Equation (5-11.52).
[20] W. E. Acree, *J. Colloid Interface Sci.* **1984**, *101*, 575–576.
[21] T. Smith, *J. Colloid Interface Sci.* **1980**, *75*, 51–55.
[22] J. Yang, J. Duan, *J. Phys. Chem. B* **2003**, *107*, 6139–6147.
[23] M. Holmberg, A. Kuhle, J. Garnaes, K. A. Morch, A. Boisen, *Langmuir* **2003**, *19*, 10510–10513.
[24] P. E. Lammert, J. Prost and R. Bruinsma, *J. Theor. Biol.* **1996**, *178*, 387–391.
[25] Platinum/gold surfaces take on a negative charge (~-40 mV) in deionized water, requiring protons from solution to balance the surface charge to preserve electroneutrality of the bulk suspension.
[26] The one-dimensional surface conductivity coefficient can be found using the Bikerman equation: $K^{od}=\sqrt{8\varepsilon_0\varepsilon cRT}\left(\frac{u_+}{A-1}-\frac{u_-}{A+1}+\frac{4\varepsilon_0\varepsilon cRT}{\mu z F}\frac{1}{(A^2-1)}\right)$ in which $A=\coth(-zF\zeta/4RT)$. Because this conductivity occurs throughout the double-layer, the resulting two-dimensional conductivity is $\sigma_d=K^{od}/\lambda_d$. This, however, disregards the conductivity of the stagnant part of the double layer which may have conductivity as much as 5–10 times higher than the diffuse layer (see Lyklema, *Fundamentals of Interface and Colloid Science*, *Vol. 2*, Academic Press, San Diego, **1991**, section 4.3f). Neglecting the contribution from the stagnant layer for simplicity, the conductivity of the diffuse layer in pure water is on the order of $10^{-5}\,S\,m^{-1}$.
[27] L. Carrette, K. A. Friedrich, U. Stimming, *Fuel Cells* **2001**, *1*, 5–39.
[28] Y. Kiros, *J. Electrochem. Soc.* **1996**, *143*, 2152–2157.
[29] Y. Kiros, S. Schwartz, *J. Power Sources* **2000**, *87*, 101–105.
[30] K. A. Friedrich, K.-G. Geyzers, U. Linke, U. Stimming, J. Stumper, *J. Electroanal. Chem.* **1996**, *402*, 123–128.
[31] S. Franz, P. L. Cavallotti, M. Bestetti, V. Sirtori, L. Lombardi, *J. Magn. Magn. Mater.* **2004**, *272–276*, 2430–2431.
[32] Z. D. Wei, S. H. Chan, *J. Electroanal. Chem.* **2004**, *569*, 23–33.
[33] The product of the rod velocity ($\sim 10\,\mu m\,s^{-1}$) and drag force (5×10^{-2} pN) gives the mechanical power dissipated by the rod as it moves through the solution, which is on the order of 5×10^{-19} W. The input power (2×10^{-10} W) can be calculated from the oxygen generation rate ($\sim 1\times 10^{-15}\,mol\,s^{-1}$) at the rod surface and the free energy change of the reaction ($-234\,kJ\,mol^{-1}$).
[34] a) T. R. Kline, W. F. Paxton, T. E. Mallouk, A. Sen, *Angew. Chem.* **2005**, *117*, 754–756; b) T. R. Kline, W. F. Paxton, T. E. Mallouk, A. Sen, *Angew. Chem.* **2005**, *117*, 754–756; *Angew. Chem. Int. Ed.* **2005**, *44*, 744–746.
[35] J. M. Catchmark, S. Subramanian, A. Sen, *Small* **2005**, *1*, 202–206.
[36] D. Pantaloni, C. Le Clainche, M.-F. Carlier, *Science* **2001**, *292*, 1502–1506.
[37] J. B. Waterbury, J. M. Willey, D. G. Franks, F. W. Valois, S. W. Watson, *Science* **1985**, *230*, 74–76.
[38] H. Lee, A. M. Purdon, V. Chu, R. M. Westervelt, *Nano Lett.* **2004**, *4*, 995–998.
[39] D. A. Brown, H. C. Berg, *Proc. Natl. Acad. Sci. USA* **1974**, *71*, 1388–1392.
[40] A. K. Salem, J. Chao, K. W. Leong, P. C. Searson, *Adv. Mater.* **2004**, *16*, 268–271.
[41] a) J. K. N. Mbindyo, B. D. Reiss, B. R. Martin, C. D. Keating, M. J. Natan, T. E. Mallouk, *Adv. Mater.* **2001**, *13*, 249–254; b) B. D. Reiss, J. K. N. Mbindyo, B. R. Martin, S. R. Nicewarner, T. E. Mallouk, M. J. Natan, C. D. Keating, *MRS Symposium Proceedings*, **2001**, *635* (Anisotropic Nanoparticles), C6.2/1–C6.2/6.
[42] S. Park, J.-H. Lim, S.-W. Chung, and C. A. Mirkin, *Science* **2004**, *303*, 348–351.

Published online: July 29, 2005

 © 2005 Wiley-VCH Verlag GmbH & Co. KGaA, Weinheim